Observation of bistable density transitions in magnetized plasma by voltage-biased electrode

Shunjiro Shinohara[a] and Shoichiro Matsuyama
Interdisciplinary Graduate School of Engineering Sciences, Kyushu University, Kasuga Koen 6-1, Kasuga, Fukuoka 816-8580, Japan

(Received 23 April 2002; accepted 28 August 2002)

Repeated transition phenomena with abrupt reductions and jumps of the electron density were observed (flip–flop pattern in bistable systems), by voltage biasing to an inserted electrode in the inner region of a rf- (radio frequency-) produced, cylindrical magnetized plasma. These global, self-excited, density transitions and back ones between two states were accompanied by changes of the floating potential profile and the bias current under various parameters. Control of the staying time probability in one of two states with hysteresis loops was attempted, changing the bias voltage, which showed the importance of a sheath region as well as fine structural patterns. © *2002 American Institute of Physics.* [DOI: 10.1063/1.1516217]

I. INTRODUCTION

The control of plasma generation and sustainment under stable conditions in time and space is one of the critical issues in the fields of plasma application, high-temperature plasma, and space plasma. The obtained plasma profile is nonlinearly governed by the balance between the plasma generation and diffusion mechanisms, and induced instabilities are closely related to the obtained profile in a complex form. The structural formation of electric fields and a bifurcation, e.g., in a nuclear fusion field, have been major concerns. These are related to the changes of plasma confinement such as a transition from the L (low) mode to the H (high) mode in tokamaks[1] with the shear of the so-called **E×B** rotation. Experiments on this transition and profile change using voltage biasing[2] were also conducted in mirror machines,[3–9] and an oscillatory transition of density and potential was discovered, e.g., in the Compact Helical System (CHS).[10] In addition, hystereses and mode changes (and sometimes chaotic behavior) in various dc and rf discharges including sheath regions, e.g., Refs. 11–19, were found on changing input voltage or input power, and these interesting characteristics arise from the inherent plasma nonlinearity. However, there have been few experiments[5–9] conducted from a basic viewpoint to study these transitions as well as to control the density and rotation profiles by imposing electric fields externally. These are connected with the transport characteristics and structure formation, and also with a further development of the application fields. Recently, density transitions in bistable systems (flip–flop pattern) were clearly found and briefly reported,[20] by voltage biasing to electrodes inserted into the rf-produced, cylindrical magnetized plasma.

Here, in this paper, we have examined, in much more detail, global characteristics of a self-excited bistable system, i.e., density transitions and back ones (oscillatory behaviors) between two states, accompanied by potential changes, using the former voltage biasing.[20] Furthermore, we could control the staying time, i.e., residence time, and staying probability in one of two states, by changing the bias voltage, with also emphasizing hysteresis characteristics in a statistical (stochastic) sense. Note that compared with observed phenomena in dc discharges reported in Refs. 11 and 13–16, our experimental conditions and findings are quite different in terms of the following points.

(1) Plasma was produced by an external rf power supply, and bistable conditions were controlled by voltage biasing to an electrode, i.e., production and control methods were independent in our case (both production and control were carried out by applying a dc discharge voltage between electrodes).
(2) Mostly, electron flow was along the magnetic field and ion flow was across the field with positive biasing, and the role of azimuthal direction such as in the case of a flow shear has been unclear up to now. Namely, a two- or three-dimensional analysis is necessary (only a one-dimensional analysis was considered, e.g., electron and ion flows between the electrodes).
(3) Bistable states were found in both increasing and decreasing phases of applied voltage (oscillations were found in the decreasing phase only in the temperature limited mode, and large fluctuations were observed when bistable states were formed).
(4) Clear bistable phenomena, e.g., staying time in one of two states was long up to more than 10 seconds while typical transition time is 1–2 ms (mostly oscillations between two states were found with small staying time, and even in one state, plasma parameters were not constant).
(5) Hysteresis characteristics were found stochastically such as mean staying time and staying time probability in a bistable system (hysteresis was found in dc current–voltage characteristics).
(6) The control of staying time and staying probability was attempted (there were a few trials).

[a]Electronic mail: sinohara@aees.kyushu-u.ac.jp

Therefore, our new findings can contribute to the understanding of relaxation/phase change phenomena (balance and triggering processes) in the basic (plasma) physics. These may also lead to a further development of application studies including nuclear fusion due to the common physics involved. This paper is organized as follows. In Sec. II we describe the experimental system, e.g., production scheme, voltage biasing system, and diagnostics in a cylindrical magnetized plasma. Experimental results on various transition phenomena in a bistable system are discussed in Sec. III for changing bias voltage, fill pressure, and rf input power. Here, after describing the typical transition phenomenon as a function of time under the various positions, global structural changes such as ion saturation current and floating potential including characteristics of fluctuations, are reported, changing one of the control parameters of bias voltage: three phases of state I only, transitions between state I and state II, and state II only. Then, operating pressure is reported, considering the boundaries of bias voltage in the above three phases and average staying time during transitions: With the increase in a pressure, both typical bias voltage and width of this voltage region to undergo transitions decreased. On the other hand, there was a large change of staying time, e.g., by three orders of magnitude, with fill pressure less than ~ 5 mTorr, and it took a minimum time at ~ 2.5 mTorr. Characteristics of hystereses of ion saturation current, staying time, and staying probability in a stochastic sense are also described for changing bias voltage. Probability distribution function of ion saturation current, and bias current behavior in a Lissajous figure were studied: the fine structure pattern from the distribution function, and the sheath effect due to the faster rise of bias current were suggested. Finally, in Sec. IV, we discuss characteristics of bistable phenomena in detail focusing on triggering/governing mechanisms of transitions, and the conclusion is given.

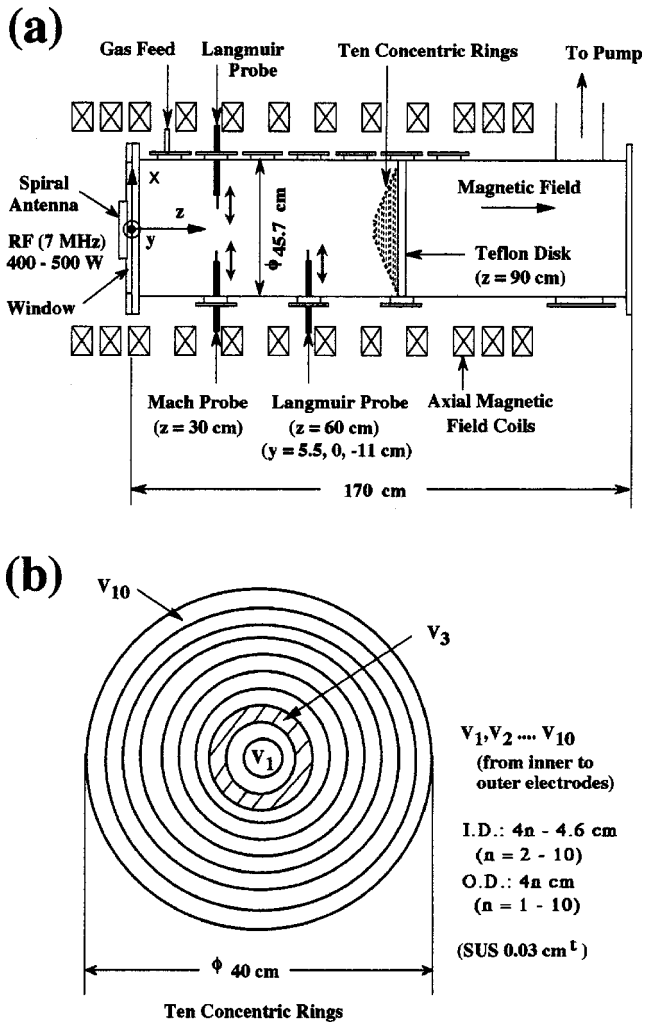

FIG. 1. Schematic view of (a) experimental setup and (b) biased electrodes with ten concentric, segmented rings.

II. EXPERIMENTAL SETUP

Argon plasma was produced by a four-turn spiral antenna[21] at a pressure of $P_0 = 0.1-10$ mTorr. The continuous output rf power and frequency of $P_{rf} = 160-500$ W and $f_{rf} = 7$ MHz, respectively, were applied to a linear device, 45 cm in diameter and 170 cm in axial length, with the uniform magnetic field of $B = 500$ G, as shown in Fig. 1(a). Here, (x, y, z) coordinates in the cylindrical system are shown. In order to control the radial potential profile, we used ten concentric, segmented rings, made of stainless steel with a thickness of 0.03 cm, as biased electrodes[6,7,9] [see Fig. 1(a) (in the middle) and Fig. 1(b)]. The inner and outer diameters of the n-th ring (in order from the center) were $4n-4.6$ cm $(2 \leqslant n \leqslant 10)$ and $4n$ cm $(1 \leqslant n \leqslant 10)$, respectively. Each ring was separated from the neighboring ones with an axial distance of 1.3 cm. These rings were placed on the Teflon™ disk, 40 cm in diameter, at the axial direction of $z = 90$ cm from the window, which was located on the left-hand side in Fig. 1(a), to cover the plasma cross section. Mostly, the No. 3 electrode (the radius is 3.7–6 cm) was used in the present experiment [see the shaded region in Fig. 1(b)].

The spatial plasma parameters, such as the plasma density, electron temperature, floating potential, and flow velocity, were measured by scanning the Langmuir probes including the Mach probe, which were located at $z = 30$ cm and 60 cm. The typical target (before biasing) plasma density n_e was in the range of $4 \times 10^9 - 4 \times 10^{10}$ cm^{-3} with the electron temperature $T_e = 3-6$ eV and estimated ion temperature < 1 eV. Here, the ion Larmor radius was less than 1 cm, and thus ions and electrons were magnetized.

III. EXPERIMENTAL RESULTS

A. Change of spatial structure during transitions (low rf power)

Figure 2 shows an example of the time evolution of the ion saturation current I_{is} measured at about one half radius of the chamber $(x = -10$ cm), on changing bias voltage V_3 (voltage at the No. 3 electrode). Here, $P_0 = 3.2$ mTorr and $P_{rf} = 160$ W, and seven traces show different shots. For the case of low bias voltage (less than 110 V), no n_e change was observed (state I) with a relative amplitude of fluctuations of less than 10%, typically. Here, n_e is considered to be nearly proportional to I_{is} since T_e did not change appreciably, and

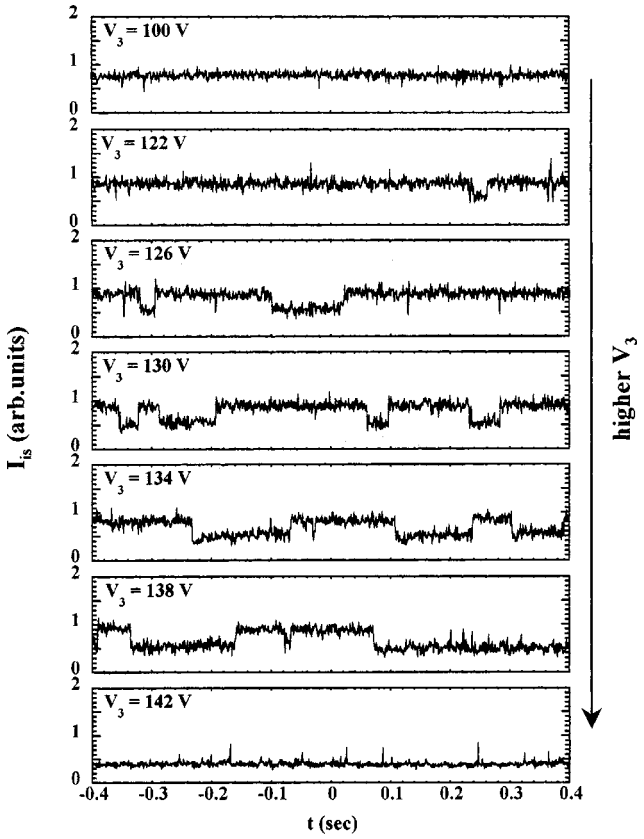

FIG. 2. Time evolution of ion saturation current I_{is} at $x=-10$ cm, changing bias voltage V_3 ($P_0=3.2$ mTorr and $P_{rf}=160$ W). Here, seven individual traces have different shots.

$I_{is}=1$ corresponded to $n_e=5.8\times10^9$ cm^{-3} for the case of $T_e=5$ eV. From this figure, with the increase in V_3, an increased number of transitions from the higher (state I) to the lower (state II) states were found, in addition to back transitions from state II to state I: density oscillation (self-excited transitions) between two states (bistable system). The typical transition time (rise and decay time between two states) was 1–2 ms. Note that for a clear bistable system with a relatively small amplitude of fluctuations, it was observed that the staying time of one state of more than several tens of ms is much larger than the transition time, which was different from the cases for the oscillations observed in dc discharges, as was discussed in the Introduction part. Finally, with a further increase in V_3 ($\geqslant 140$ V), there appeared a lower n_e state, which is stationary with time, i.e., the state II only, with neither back transitions to the state I nor any events of arcs.

During a transition, global profile changes in the radial direction were found, as shown in Fig. 3 (the same condition as in Fig. 2). For the case of the floating potential with respect to the electrode No. 3 with other electrodes also being at a floating potential, a hollow radial profile of the floating potential V_f and density peaking were observed (note that Figs. 3 and 4 were drawn in a region of $x=-22\sim5$ cm). In the outer region of the biased electrode for the case of $V_3=130$ V, both n_e and V_f decreased in a transition from state I to state II by up to 60% and 12 V, respectively. Here, the electrode position is denoted by the closed horizontal bar in Figs. 3–5, where a dip of n_e near this electrode was observed

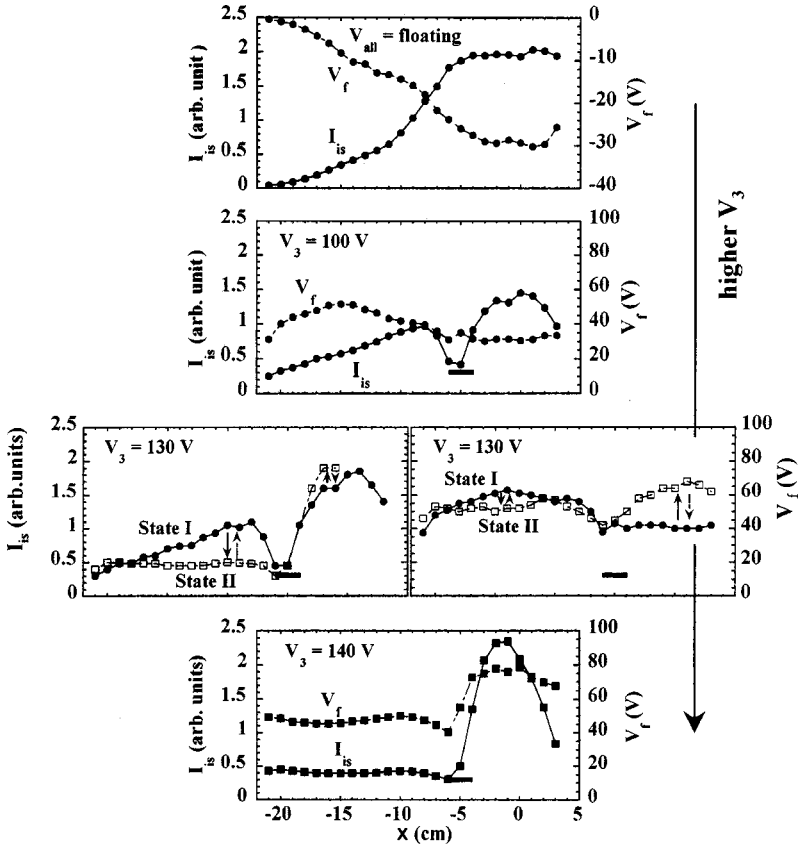

FIG. 3. Radial profiles of ion saturation current I_{is} and floating potential V_f, for changing bias voltage V_3 ($P_0=3.2$ mTorr and $P_{rf}=160$ W). Here, state I and state II (closed circles and open boxes, respectively) are shown in the third figures from the top, and radial position of the No. 3 electrode is denoted by a horizontal closed bar.

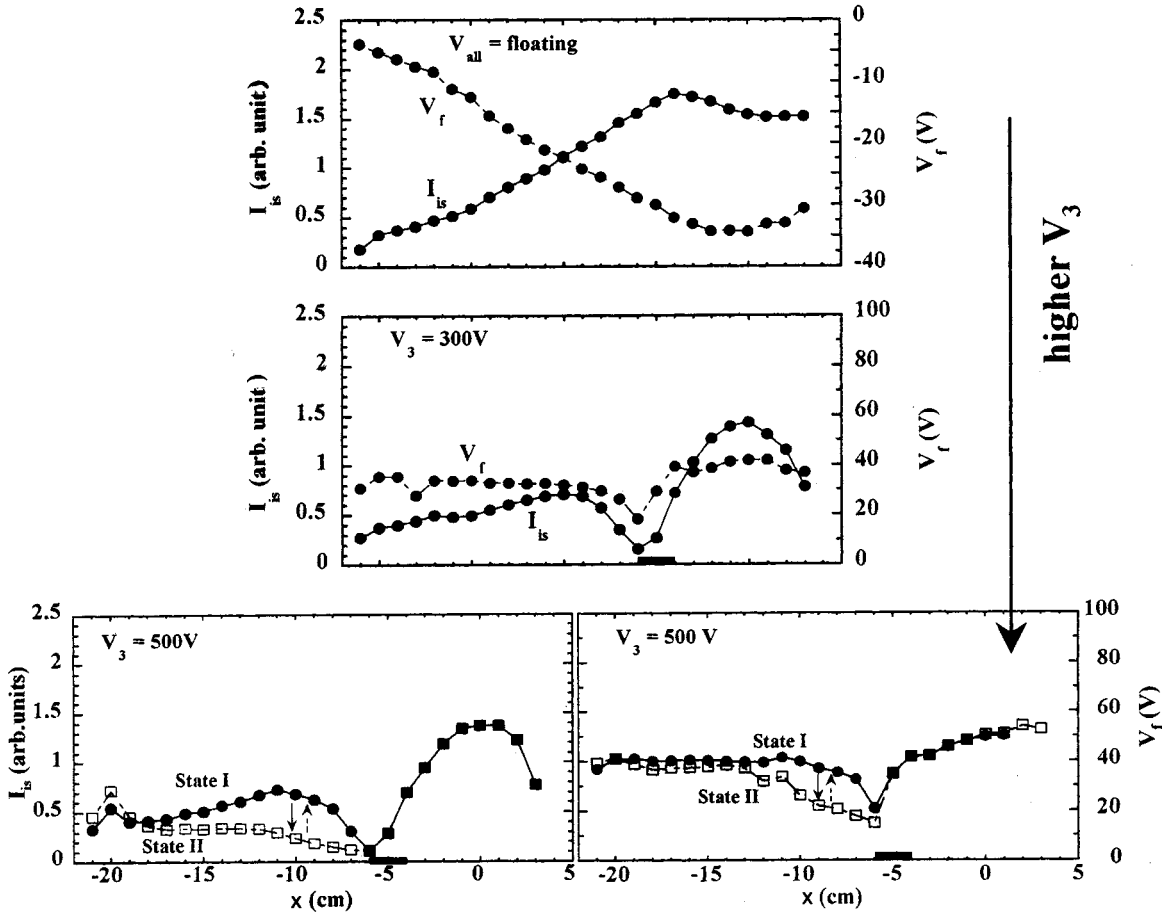

FIG. 4. Radial profiles of ion saturation current I_{is} and floating potential V_f, for changing bias voltage V_3 ($P_0=0.64$ mTorr and $P_{rf}=160$ W).

due to the parallel electron current along the magnetic field.[5–7,9]

In the inner region, changes of n_e and V_f behaved in opposite ways (Fig. 3): n_e and V_f increased (by up to 30 V) after a transition to state II. Here, profiles in state I (II) with $V_3=130$ V correspond well with those with a lower (higher) bias voltage than 130 V where no transitions were observed. However, from changes of n_e and V_f, the Boltzmann's relation was not found at the same position as well as along the radial direction. Concerning density fluctuations, except for the central plasma region, odd number modes m (probably the $m=1$ mode) along the azimuthal direction dominated. Although the relative fluctuation amplitude in the inner region of the electrode did not change appreciably during a transition, this relative amplitude from state I to state II decreased by up to more than a factor of 2 in the outer region.

With the lower fill pressure of 0.64 mTorr keeping the same input rf power, similar behaviors of global spatial changes of n_e and V_f during a transition were found, as shown in Fig. 4: n_e and V_f decreased by up to 75% and 20 V, respectively, from state I to state II, and both n_e and V_f underwent transitions at nearly the same time along the radial direction (a simultaneous global change). However, transition phenomena at $P_0=0.64$ mTorr were found to occur at the higher V_3 voltage region than those at $P_0=3.2$ mTorr (see Fig. 7 below), and changes of I_{is} and V_f were negligibly small in the inner radial region of the No. 3 electrode compared to those in the outer region.

B. Change of spatial structure during transitions (low pressure and high rf power)

Compared to Figs. 3 and 4, n_e (V_f) decreased (increased) in the outer region during a transition from state I to state II, for the case of the lower pressure with the higher rf power, e.g., $P_0=0.16$ mTorr and $P_{rf}=400$ W, as shown in Fig. 5. Here, error bars (long error bars on the negative side) show the amplitude of fluctuations (negative spikes), instead of statistical error bars normally used. The density transition suddenly occurred from state I, whose typical staying time (residence time) was very long and larger than one minute, with giant oscillations of density to state II with small fluctuations or vice versa, as shown in Fig. 6 (back transitions occurred after one minute or more from state II to state I with the enhancement of fluctuations). Here, state I had a typical fluctuation frequency $f=1-2$ kHz (this fundamental frequency sometimes has its second harmonic) with the $m=1$ mode in the outer region and even m numbers in the inner one. On the other hand, state II had a broad spectrum of $f=2-5$ kHz in the outer region of a biased electrode [see error bars (fluctuation amplitude) in Fig. 5 and oscillations as a function of time in Fig. 6]. Once this transition took place,

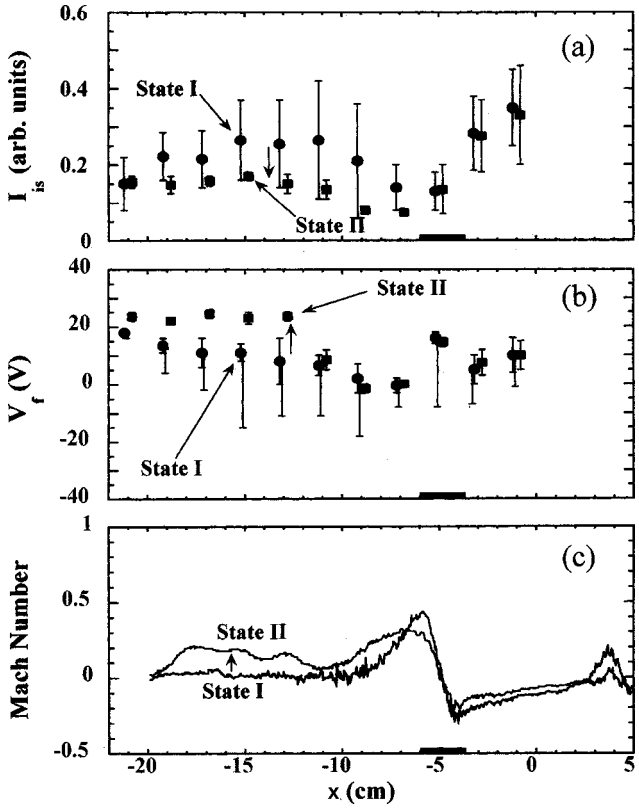

FIG. 5. Radial profiles of ion saturation current I_{is}, floating potential V_f and Mach number at state I and state II ($V_3=200$ V, $P_0=0.16$ mTorr, and $P_{rf}=400$ W). Here, error bars (long error bars in the negative side) show the amplitude of fluctuations (negative spikes).

state II remained for a long time (more than a few minutes as was mentioned) with almost no back transitions to state I in the observation period of less than a few minutes. For the case of floating bias, the typical fluctuation frequency was low, ~ 1 kHz, with a smaller amplitude than that at state I. Concerning fluctuations of V_f, this signal sometimes showed sawtooth-like behavior as a function of time, and density fluctuations observed may be considered as drift waves, which were also found in the previous experiments of voltage biasing (density profile change and formation of velocity shear).[7,9]

This phenomenon and a profile change of V_f during a transition, i.e., an increase in V_f from state I and state II in the outer region, are different from the above-mentioned transitions with low-power and high-pressure conditions. From the Mach probe measurement, as shown in Fig. 5(c), plasma rotated in the azimuthal direction in a rigid body like near the electrode, i.e., the rotation speed is proportional to the radial distance from the electrode with opposite signs on both sides (inner and outer regions), and the absolute, maximum Mach number M was less than 0.5. However, this speed is higher (lower) near (far from) the electrode at state I than at state II. Here, M is defined as rotation velocity divided by the ion sound velocity, and a positive value of M indicates a rotation in the ion diamagnetic direction. In estimating the Mach velocity, for convenience,[6–9,22] an unmagnetized model[23] or a kinetic model[24] with zero viscosity was employed. Note that this observed speed was lower than those in the previous experiments, where drift waves were observed,[7,9] and was much lower than that in the rotation plasma, where velocity shear driven instabilities were observed.[25]

C. Operating pressure region

Figure 7 shows the characteristics of transitions as a function of fill pressure keeping $P_{rf}=160$ W; bias voltage V_3 and average staying time at state II were measured. Here, closed circles, open triangles and closed boxes show, respectively, points of the onset from state I to state II, points of 50% staying probability (of time) for each state, and points of the onset of full transitions to state II. Average staying time T_{aII} in Fig. 7(b) is defined as the total staying time at state II divided by frequency (number of events) during the observation time, for the case of 50% staying probability for both states I and II. This T_{aII} was derived under the same condition as those shown by open triangles in Fig. 7(a). Note that data were taken for the increasing phase of the bias voltage V_3 (see descriptions of hystereses in Figs. 8–11 below obtained by changing V_3). From this figure, with the increase in pressure, both typical V_3 voltage and width of V_3 region undergo transitions (vertical distance between a closed circle and a closed box) decreased. On the other hand, with the increase in P_0, T_{aII} decreased with P_0 from ~ 15 sec at $P_0 \sim 0.6$ mTorr and had the minimum of ~ 20 ms at $P_0 \sim 2.5$ mTorr (this was much smaller by three orders of magnitude than that at $P_0 \sim 0.6$ mTorr). Then, with a further increase in P_0, T_{aII} increased slowly to ~ 200 ms at $P_0 \sim 5$ mTorr. Here, transitions became negligible at more than 5 mTorr. Although this curve of T_{aII} in Fig. 7 has not been explained so far, this behavior seems to be similar to that described by the Paschen's law (needless to say, staying time is different from a discharge voltage), but expected pressure at the minimum point estimated based on typical device size is larger than the observed pressure by one order of magnitude. Here, at $P_0 \sim 2.5$ mTorr, where there seemed to be a boundary of two regions as to average staying time, the electron mean free path (mainly dominated by electron-neutral collisions) is about one half of the plasma radius.

With increasing P_{rf}, while maintaining a constant value of P_0, the required bias voltage V_3 leading to a transition between state I and state II decreased, and thus for the case of constant V_3, staying probability and average staying time at state II increased. In the present experiment described so far, data were obtained by the use of a No. 3 electrode only, but density transitions were also observed on changing the position of a bias electrode; application of a bias voltage to an individual electrode from Nos. 1–9 (positions are shown in Fig. 1) caused similar behaviors.

D. Hysteresis characteristics

In order to examine hysteresis characteristics stochastically, ion saturation current I_{is} was measured by, first, increasing V_3 slowly in a continuous manner from the lower voltage region where there were no density transitions from state I to state II, to the higher one having no back transitions from state II to state I, through self-excited transitions be-

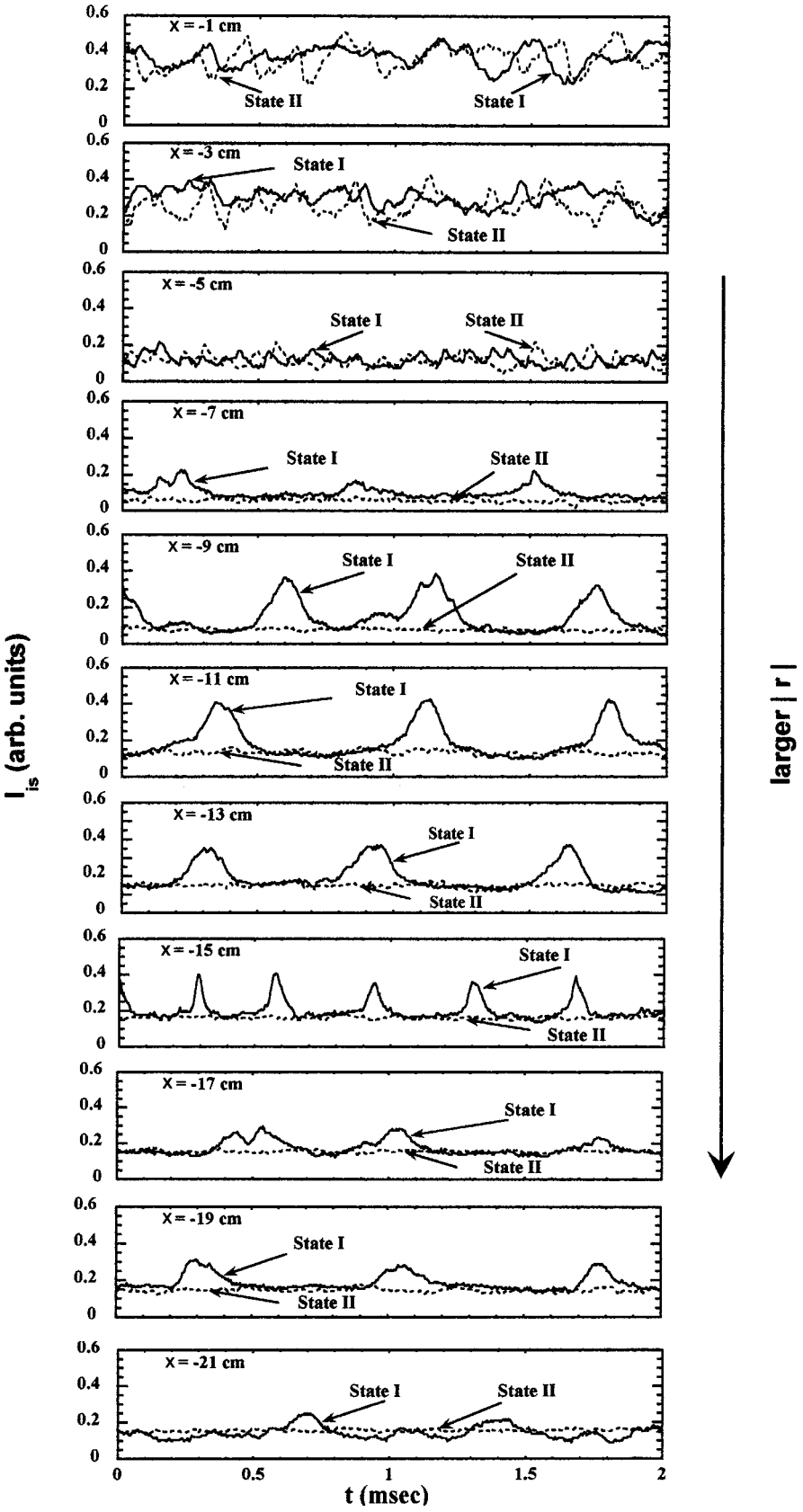

FIG. 6. Time evolution of ion saturation current I_{is} at state I and state II, at $x=-1$ cm~-21 cm (every 2 cm) from top to bottom ($V_3=200$ V, $P_0=0.16$ mTorr, and $P_{rf}=400$ W). Here, 22 individual traces have different shots.

tween two states. Next, reducing V_3 in the opposite manner from the high voltage region for the case of only state II to the low voltage for state I alone. This voltage change of V_3, i.e., up and down, was conducted continuously without termination of the plasma, keeping external parameters constant (the wall effect was also determined to change orders of phases of increasing and decreasing voltages). Note that the time of changing V_3 to measure plasma parameters ranged

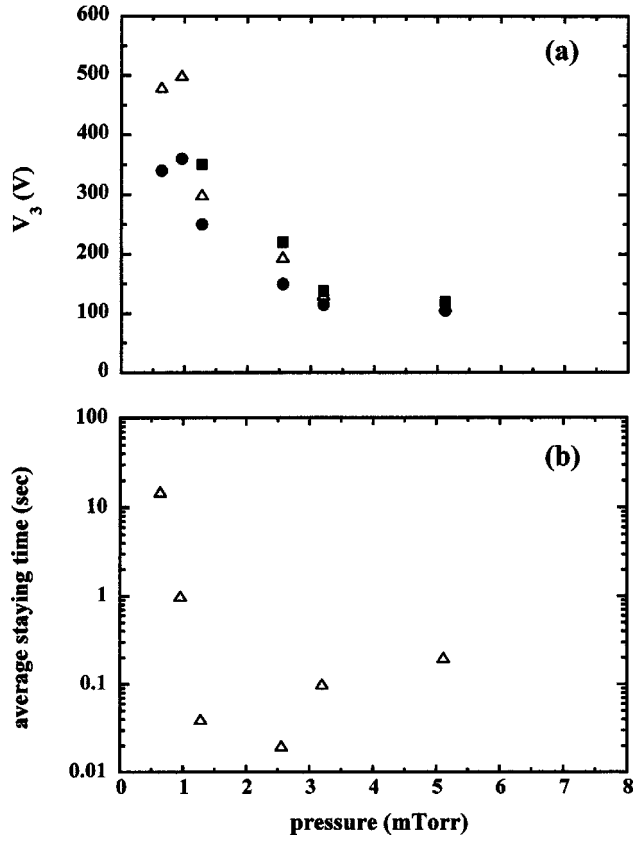

FIG. 7. (a) Bias voltage V_3 and (b) average staying time at state II as a function of fill pressure measured at $x=-10$ cm ($P_{rf}=160$ W). Here, closed circles, open triangles, and closed boxes show, respectively, points of the onset from state I to state II, points of 50% staying probability (time) for each state, and points of onset of full transitions to state II. The average staying time in Fig. 7(b) is defined as the total staying time divided by frequency for the case of 50% staying probability for both states.

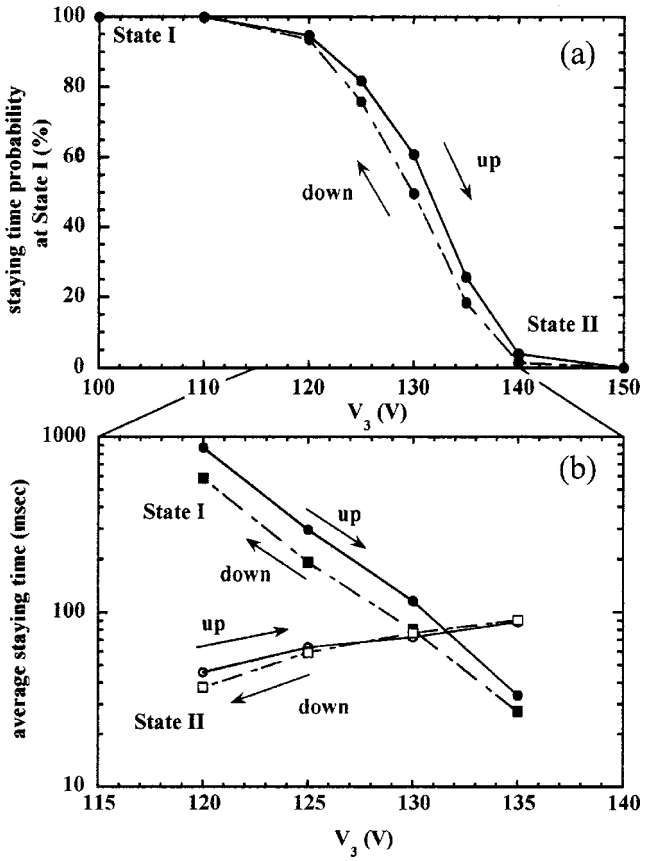

FIG. 9. Hysteresis curves of (a) staying time probability at state I and (b) average staying time for state I and state II, from data of the ion saturation current measured at $x=-10$ cm, as a function of bias voltage V_3 ($P_0=3.2$ mTorr and $P_{rf}=160$ W). Here, the staying time probability is defined as the total staying time at state I divided by the total measuring time, and the average staying time is defined as the total staying time at each state divided by frequency.

from tens of seconds to several minutes depending on the average staying time (see Fig. 7). Figure 8 shows clear hysteresis curves of the relationship between I_{is} and V_3 obtained by the above-mentioned method ($P_0=3.6$ mTorr and $P_{rf}=160$ W). Here, each curve in this figure was derived by averaging six data (six curves), and I_{is} is the weighted (time) average of different values of I_{is} at state I and state II (see, e.g., Fig. 2) for $V_3=130$ V to 160 V. This is completely different from the hysteresis curve, i.e., current–voltage characteristics, for dc discharges discussed in the Introduction.

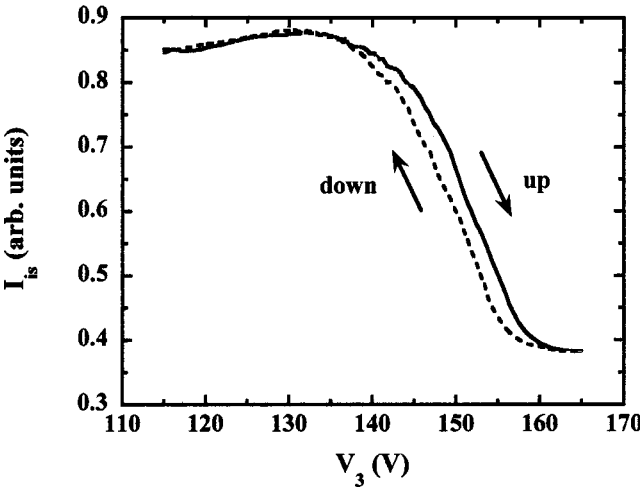

FIG. 8. Hysteresis curves of averaged ion saturation current I_{is} at $x=-10$ cm as a function of bias voltage V_3 ($P_0=3.6$ mTorr and $P_{rf}=160$ W).

This hysteresis characteristic was ascertained in another way: Staying time probability P_s, defined as the ratio of the time occupied at state I normalized by total observation time, is shown in Fig. 9(a) (the same conditions as those in Figs. 2 and 3). Below $V_3\sim 110$ V, plasma had state I all the time, and this probability at state I decreased with increasing V_3, and finally only state II existed by high voltage biasing above 140 V. The threshold voltages of no transitions from state I and state II, i.e., on the margin of 100% staying probability at state I and state II, were higher for the case of increasing phases of V_3 than for the case of decreasing phases (see the low- and high-voltage regions of 110–120 V and 140–150 V, respectively, and also see Figs. 8–10). Figure 9(b) shows the average staying time $T_{aI}(T_{aII})$, defined as the total staying time at state I (II) divided by frequency during observation time. While T_{aI} decreased rapidly with V_3 by more than one order of magnitude, T_{aII} and the variance

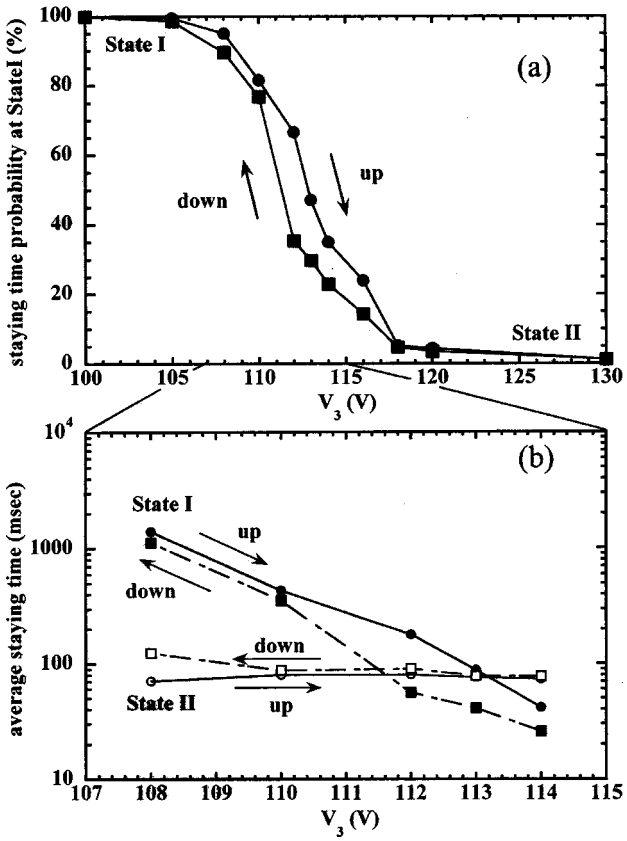

FIG. 10. Hysteresis curves of (a) staying time probability at state I and (b) average staying time for state I and state II, from data of the ion saturation current measured at $x=-10$ cm, as a function of bias voltage V_3 ($P_0=5.1$ mTorr and $P_{rf}=160$ W).

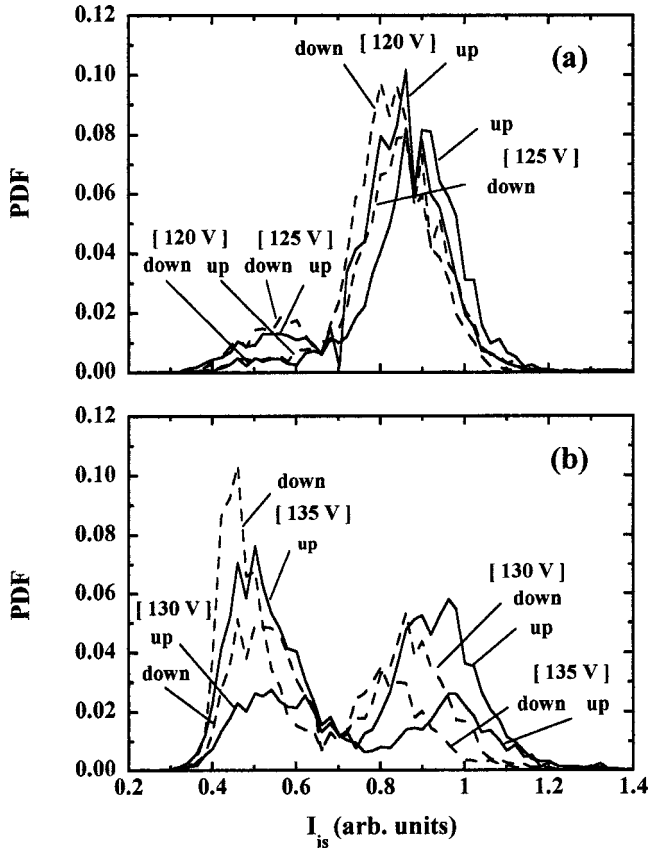

FIG. 11. Probability distribution as a function of ion saturation current I_{is} at $x=-10$ cm, for increasing (up) and decreasing (down) phases of bias voltage V_3: (a) 120 V and 125 V and (b) 130 V and 135 V ($P_0=3.2$ mTorr and $P_{rf}=160$ W).

of staying time at state II (not shown) increased slowly with V_3. Hysteresis loops were found for both staying time probability and the average staying time from Fig. 9: P_s and T_{aI} were higher with phases of increasing V_3 (up) than those of decreasing V_3 (down) for the same value of V_3 (a slight difference was found for T_{aII} behavior). On changing fill pressure, the same phenomena concerning P_s, T_{aI}, and T_{aII} were observed, and another example is shown in Fig. 10 for the case of $P_0=5.1$ mTorr. From this figure, the V_3 region for self-excited transitions was lower than that in Fig. 9 due to the increase in P_0 as was discussed in Fig. 7.

E. Detailed structure

We have attempted to observe the fine structure and hysteresis behavior stochastically: the ion saturation current I_{is} as a function of the bias voltage V_3, e.g., a probability distribution of I_{is} (PDF), was plotted, as shown in Fig. 11, for increasing (up) and decreasing (down) phases of bias voltage V_3 between 120 V and 135 V. Here, the interval of I_{is} to plot the distribution in this figure was taken as ~ 0.02, with the total number of data points of 32000 (original data have 8 bit resolution). From Fig. 11, in the increasing phase of V_3, there was a tendency, particularly for the case of the high bias voltage, that the probability to have state I (state II) was higher (lower) than that in the decreasing phase of V_3, which is consistent with Figs. 8–10. In addition, central values of I_{is} at state I (the higher side of the I_{is} value from two main peaks in this figure, for the case of $V_3=120-135$ V) and state II (the lower side for the case of $V_3=135$ V) were larger in the increasing phase of V_3 than in the decreasing phase. The hysteresis characteristics obtained from Figs. 8–10 along with the results in Fig. 11 may come from the fine spatial structure change between increasing and decreasing phases, in addition to those from other hidden parameters, or from some memory effects, which should be clarified in future studies.

In order to determine the triggering process of transitions, the time of transitions of various parameters was measured. There were neither a clear difference of times between I_{is} and V_f during a transition, nor a significant difference of time between measuring radial positions of both I_{is} and V_f. However, the bias current I_b on the order of 10 mA at the No. 3 electrode increased fast just before or near the same time of density transitions from state I to state II; fast I_b rise with an overshot positive spike was found while I_{is} drop was slow, as shown in Fig. 12(a) (sampling time was 200 μs). Here, a positive value shows that electrons (ions) are flowing into (out from) the electrode, and changes of V_3 and P_{rf} were less than 1% during a transition. The differences of time and timescale are clearly seen in the Lissajous figure in Fig. 12(b), which shows a relation between I_{is} and I_b replotted from Fig. 12(a). On the back transition from state II to state

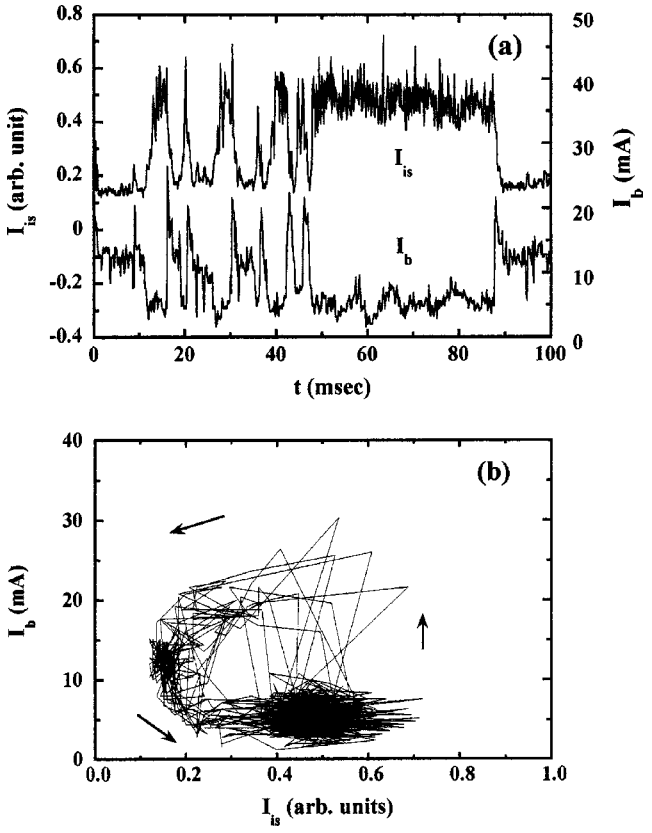

FIG. 12. (a) Time evolution of ion saturation current I_{is} at $x=-17$ cm and bias current I_b, and (b) Lissajous figure between I_{is} and I_b taken from (a) ($V_3=200$ V, $P_0=1.6$ mTorr, and $P_{rf}=160$ W).

I, I_b decrease was also faster than I_{is} increase. From our measurements conducted so far, only the change of I_b was seen to be earlier than other signals during a transition among the measured signals, which indicates the importance of changing parameters in the neighboring region (sheath region) of the bias electrode for triggering a transition process.

IV. DISCUSSION AND CONCLUSION

Here, we will discuss characteristics of bistable phenomena while focusing on triggering/governing mechanisms of transitions. Generally, transitions in this bistable system may be understood phenomenologically based on the effective, asymmetric double well potential structure, e.g., Ginzburg–Landau equation, or Schmitt trigger[26] (obtained results may also be related to stochastic resonance[26,27]); there are two stable states, whose staying probability can be varied by external parameters due to the structural modification of double well potential. Random reversal of the Earth's magnetic field is still a hot topic. The bistability and oscillations were analyzed from the context of dynamo system,[28] and governing equations of a disk dynamo model could be reduced to Lorentz equations (low-dimensional dynamics). This can also be used as an example to model our observed phenomena: random staying time or random transitions between two states depending on external parameters with fluctuations. In the CHS device, the neoclassical bifurcation curves, i.e., the electric field as a function of the electron density, were shown to explain the electric pulsation.[29] In the W7-AS device, dithering cycles (swing of hysteresis) near the threshold power for transitions from the H mode to the L mode, i.e., repeated transitions and back ones, were observed in the power flux and electron temperature gradient plane.[30] It also showed no smooth transition to improved confinement but rather the development of a barrier which suddenly appears and vanishes. In the JT-60U device, the L phase and H phase confinements appear repeatedly in a hot ion mode plasma during the almost constant input power.[31] The electron and ion temperatures were not constant in each phase, and the strong shear of the electric field contributed to reducing the thermal diffusivity. In any case, it is necessary to derive such a control plasma parameter to determine the bifurcation in our bistable system.

Although physical pictures and control parameters to describe the bistable phenomena are necessary as discussed above, due to the presence of hysteresis loops such as averages of ion saturation current, staying time probability, and staying time, as a function of bias voltage, mentioned in Sec. III D, establishment of the above pictures must be modified to explain our findings. Needless to say, if the characteristic time scale of transition is shorter (longer) than the time rate of the change of control parameters, hysteresis phenomena cannot (can) be observed, e.g., in discussing stochastic transitions between turbulent and thermodynamic branches, using control parameters as a pressure gradient[32] In our case, hysteresis loops cannot be expected on the basis of this context, since the time of changing bias voltage was chosen to be longer than the transition time and staying time. Therefore, it is necessary to find a clue to explain the results of transitions with stochastic hystereses; e.g., a search for local but not global parameters may be necessary, and the plasma parameters near the electrode must be investigated. As to the triggering parameters, from our measurements conducted so far, only a change of I_b was faster/earlier than that of other signals during a transition among measured signals such as ion saturation current and floating potential in the bulk plasma region, as was discussed in Sec. III E (see Fig. 12). Compared to the H mode transition in torus plasmas, drastic changes of floating potential profile (and thus electric field profile) as well as rotation profiles were not found in our case; a smaller rotation speed at state II than that at state I was found near the electrode in Fig. 5, but the role of flow shear has been unclear up to now. These results indicate the importance of changing parameters in the neighboring region (sheath region) of the bias electrode for triggering a transition process. This may be related to similar results that power thresholds for the L–H and H–L transitions in the ASDEX upgrade were both governed by energy flux to the separatrix region.[33]

Next, we will consider the characteristic time. Typical transition time (rise and decay time between two states) was 1–2 ms, while the average staying time in one state can be varied in a wide range, depending on the fill pressure and bias voltage, as was mentioned in Sec. III. Here, the global energy confinement time (parallel transit time along the magnetic field line by an ion sound wave passing through the

plasma) is estimated to be roughly $\sim 10\ \mu s$ ($\sim 300\ \mu s$). Collision times between electrons or between ions were shorter than the ion–neutral collision time on the order of 100 μs. These are much smaller than the transition time, but the following times are comparable to the observed transition time, if anomalous diffusivity is taken into account due to, e.g., the presence of some instabilities, as is often seen; parallel ion transit time by ion thermal velocity (characteristic time estimated by the ion classical transport across the magnetic field) is on the order of $\sim$ms (~ 10 ms). Collision time between ion and electron and pumping time were on the order of seconds, which are much larger than the transition time.

The self-oscillations in thermionic dc discharges[13–16] show three phases in one oscillation period on the order of several ms: the expansion, double layer, and relaxation phases. In this case, changes of potential structure depending on the position between the electrodes were found. In an asymmetric plasma divided by a magnetic filter, the time scale of the limit cycle numerically observed was determined by the speed of the laminar shock waves.[34] In our case, appreciable strong asymmetry and a propagation of potential change along the z axis in the bulk plasma region were not observed. Although the triggering mechanism and time scale of transition and staying time are still unclear, we must consider the potential profile modification near the electrode such as the formation of the dip (or hump) structures to change the parallel electron current (along the magnetic field), and thus, to keep the total ambipolarity, which leads to a change of the perpendicular component of ion flow due to enhanced/reduced diffusion by, e.g., change of some instabilities or turbulent states. The ion transport across the field is considered to be important in the global spatial change of plasma parameters (observed transition time becomes comparable to the ion diffusion time if an anomaly factor of several times is included as was mentioned). Needless to say, the particle balance of production and losses should be estimated in a complicated nonlinear interaction between atomic physics, plasma transport and boundary effects.

In order to understand the transition mechanisms with the hysteresis, it may be also important to determine the fine spatial structure change between increasing and decreasing phases from the PDF data of ion saturation current in Fig. 11 (the presence of sub-stable conditions is suggested as well from this figure due to an appearance of some small peaks, which is similar to the case in Ref. 29). A search for some hidden parameters including boundaries and some memory effects should be performed, and roles and couplings between the inner and outer regions separated by electrodes must be investigated in addition. We have a plan to investigate in more detail the spatio-temporal behavior of various parameters including the edge region in order to gain a full understanding of observed behaviors with some modeling. These results of transitions (phase change), relaxations, and oscillations with hystereses in a nonlinear, self-organized manner will be expected to contribute to a general important understanding of various fields of plasma physics: high-temperature plasma and other plasmas in the basic and application fields. We must note that there are some differences between the cases of our plasma and high-temperature plasma, such as the field geometry (end effects in the z direction must also be considered in our case) and ionization ratio (neutrals are also important in our system).

In conclusion, self-excited transitions between two states were investigated by the voltage biasing to an inserted electrode in the inner region of a rf-produced, magnetized plasma. Global repeated transition phenomena (flip–flop pattern) with sharp reductions and jumps of the electron density in the outer region were observed (bistable system). Transitions were accompanied by changes such as the floating potential profile and the bias current. Control of the staying time probability P_s was attempted, and hysteresis characteristics of the averaged ion saturation current I_{is}, P_s, the average staying time T_a, and a probability distribution of I_{is} were found on changing the bias voltage V_3, leading to the role of a fine structural change. During transition, the change of bias current I_b occured faster/earlier than that of other signals, which showed the importance of the sheath behavior.

ACKNOWLEDGMENT

We would like to thank Professor Y. Kawai for his continuous encouragement.

[1] K. H. Burrell, Phys. Plasmas **4**, 1499 (1997).
[2] R. J. Taylor, M. L. Brown, B. D. Frial, H. Grote, J. R. Liberati, G. J. Morales, P. Pribyl, D. Darrow, and M. Ono, Phys. Rev. Lett. **63**, 2365 (1989).
[3] A. Tsushima, T. Mieno, M. Oertl, R. Hatakeyama, and N. Sato, Phys. Rev. Lett. **56**, 1815 (1986).
[4] O. Sakai, Y. Yasaka, and R. Itatani, Phys. Rev. Lett. **70**, 4071 (1993).
[5] S. Shinohara, H. Tsuji, T. Yoshinaka, and Y. Kawai, Surf. Coat. Technol. **112**, 20 (1999).
[6] S. Shinohara, N. Matsuoka, and T. Yoshinaka, Jpn. J. Appl. Phys. **38**, 4321 (1999).
[7] S. Shinohara, N. Matsuoka, and S. Matsuyama, Trans. Fusion Technol. **39**, 358 (2001).
[8] S. Matsuyama, S. Shinohara, and O. Kaneko, Trans. Fusion Technol. **39**, 362 (2001).
[9] S. Shinohara, N. Matsuoka, and S. Matsuyama, Phys. Plasmas **8**, 1154 (2001).
[10] A. Fujisawa, H. Iguchi, H. Idei, S. Kubo, K. Matsuoka, S. Okamura, K. Tanaka, T. Minami, S. Ohdachi, S. Morita, H. Zushi, S. Lee, M. Osakabe, R. Akiyama, Y. Yoshimura, K. Toi, H. Sanuki, K. Itoh, A. Shimizu, S. Takakgi, A. Ejiri, C. Takahashi, M. Kojima, S. Hidekuma, K. Ida, S. Nishimura, M. Isobe, N. Inoue, R. Sakamoto, S.-I. Itoh, Y. Hamada, and M. Fujiwara, Phys. Rev. Lett. **81**, 2256 (1998).
[11] P. Y. Cheung and A. Y. Wong, Phys. Rev. Lett. **59**, 551 (1987).
[12] J. Hopwood, Plasma Sources Sci. Technol. **1**, 109 (1992).
[13] F. Greiner, T. Klinger, and A. Piel, Phys. Plasmas **2**, 1810 (1995).
[14] T. Klinger, F. Greiner, A. Rohde, and A. Piel, Phys. Plasmas **2**, 1822 (1995).
[15] C. Arnas Capeau, G. Prasad, G. Bachet, and F. Doveil, Phys. Plasmas **3**, 3331 (1996).
[16] Y. Ping, C. X. Yu, J. L. Xie, J. Ke, X. W. Hu, H. Li, and W. X. Ding, Phys. Plasmas **8**, 5006 (2001).
[17] S. Shinohara, Y. Miyauchi, and Y. Kawai, Plasma Phys. Controlled Fusion **37**, 1015 (1995).
[18] S. Takamura, M. Y. Ye, T. Kuwabara, and N. Ohno, Phys. Plasmas **5**, 2151 (1998).
[19] S. Shinohara and K. Yonekura, Plasma Phys. Controlled Fusion **42**, 41 (2000).
[20] S. Matsuyama and S. Shinohara, J. Plasma Fusion Res. SERIES **4**, 528 (2001).
[21] S. Shinohara, S. Takechi, N. Kaneda, and Y. Kawai, Plasma Phys. Controlled Fusion **39**, 1479 (1997).

[22]S. Shinohara, Phys. Plasmas **9**, 1834 (2002).
[23]M. Hudis and L. M. Lidsky, J. Appl. Phys. **41**, 5011 (1970).
[24]K-S. Chung, I. H. Hutchinson, B. LaBombard, and R. W. Conn, Phys. Fluids B **1**, 2229 (1989).
[25]J. R. Peñano, G. Ganguli, W. E. Amatucci, and D. N. Walker, Phys. Plasmas **5**, 4377 (1998).
[26]B. McNamara and K. Wiesenfeld, Phys. Rev. A **39**, 4854 (1989).
[27]R. Benzi, S. Sutera, and A. Vulpiani, J. Phys. A **14**, L453 (1981).
[28]K. A. Robbins, Math. Proc. Cambridge Philos. Soc. **82**, 309 (1977).
[29]A. Fujisawa, H. Iguchi, T. Minami, Y. Yoshimura, H. Sanuki, K. Itoh, M. Isobe, S. Nishimura, C. Suzuki, K. Tanaka, M. Osakabe, I. Nomura, K. Ida, S. Okamura, K. Toi, S. Kado, R. Akiyama, S. Shimizu, C. Takahashi, M. Kojima, S.-I. Itoh, K. Matsuoka, Y. Hamada, and M. Fujiwara, Phys. Plasmas **7**, 4152 (2000).
[30]U. Stroth, K. Itoh, S.-I. Itoh, H. Hartfuss, H. Laqua, the ECRH team, and the W7-AS Team, Phys. Rev. Lett. **86**, 5910 (2001).
[31]H. Shirai, M. Kikuchi, T. Takizuka, T. Fujita, Y. Koide, G. Rewoldt, D. Mikkelsen, R. Budny, W. M. Tang, Y. Kishimoto, Y. Kamada, T. Oikawa, O. Naito, T. Fukuda, N. Isei, Y. Kawano, M. Azumi, and the JT-60 Team, Nucl. Fusion **39**, 1713 (1999).
[32]M. Kawasaki, S.-I. Ito, M. Yagi, and K. Itoh, J. Phys. Soc. Jpn. **71**, 1268 (2002).
[33]H. Zohm, Plasma Phys. Controlled Fusion **38**, 105 (1996).
[34]K. Ohi, H. Naitou, Y. Tauchi, and O. Fukumasa, Phys. Plasmas **8**, 23 (2001).